Finite-volume modelling of geophysical electromagnetic data using potentials on unstructured staggered grids

Hormoz Jahandari and Colin G. Farquharson

MEMORIAL UNIVERSITY
Department of Earth Sciences
St. John's, Newfoundland, Canada

SEG 85th Annual Meeting, New Orleans

October 20, 2015

Contents

Unstructured grids

- Model irregular structures

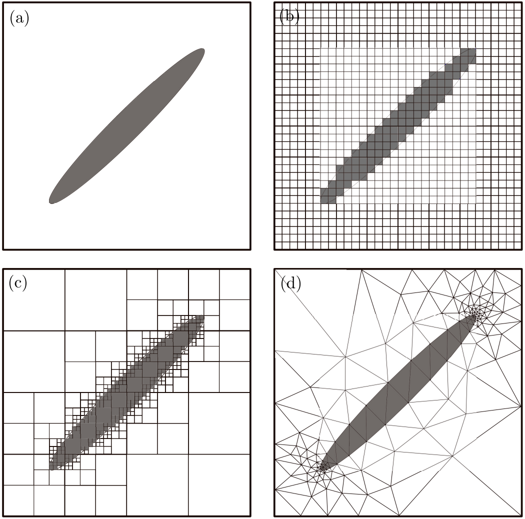

Unstructured grids

- Topographical features
- Geological interfaces
- Local refinement (at observation points, sources, interfaces)

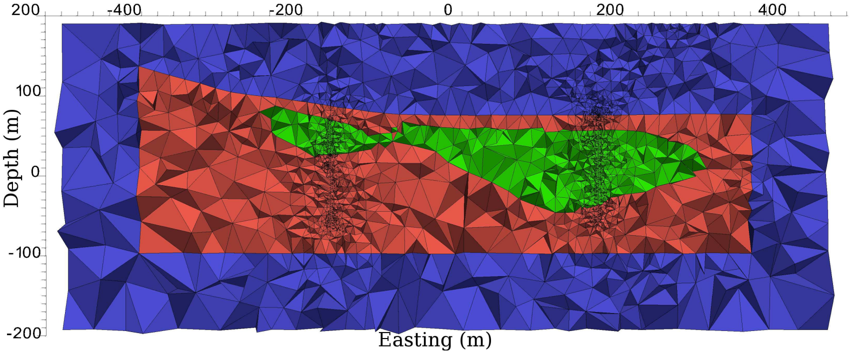

- **Grid generator: TetGen (Si, 2004)**

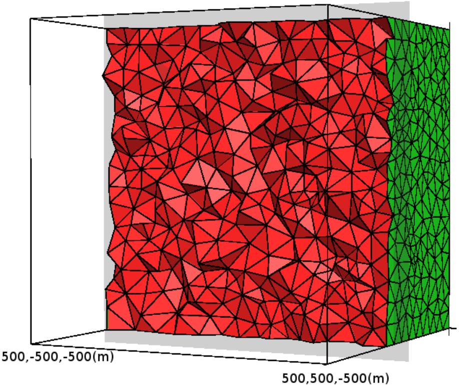

tetrahedral grid

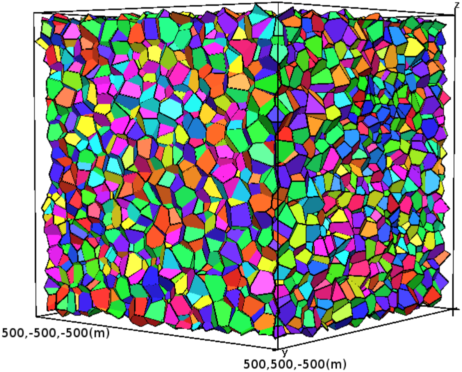

Voronoï grid

Staggered finite-volume schemes

- Magnetic field divergence free
- Easy for implementing boundary conditions
- Satisfies the continuity of tangential E
- Physically meaningful

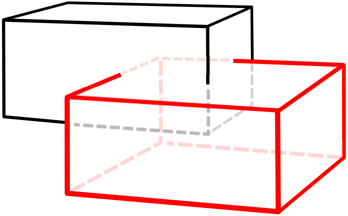

Rectilinear dual grid

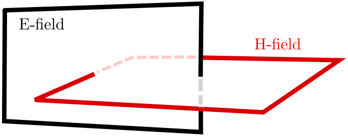

Rectilinear dual contours

Staggered finite-volume schemes

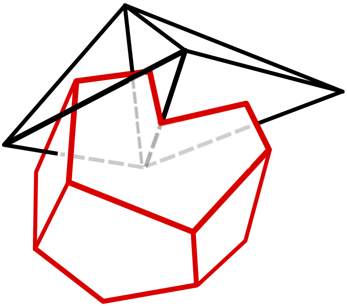

Dual tetrahedral-Voronoï grid

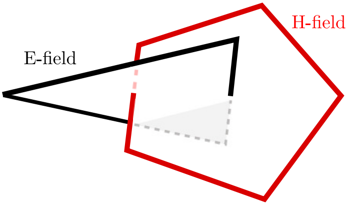

Delaunay-Voronoï contours

Staggered finite-volume schemes

Direct EM-field method

- Unknowns are E and/or H
- Simpler
- Smaller system of equations
- Ill-conditioned

EM Potential ($A - \phi$) method

- Unknowns are A and ϕ
- Larger system of equations
- Well-conditioned
- Allows studying the galvanic and inductive parts

Direct EM-field formulation of Maxwell's equations

- **Maxwell's equations:**

$$\nabla \times \mathbf{E} = -i\omega\mu_0\mathbf{H} - i\omega\mu_0\mathbf{M}_p$$
$$\nabla \times \mathbf{H} = \sigma\,\mathbf{E} + \mathbf{J}_p$$

Helmholtz equation for electric field

$$\nabla \times \nabla \times \mathbf{E} + i\omega\mu_0\sigma\mathbf{E} = -i\omega\mu_0\mathbf{J}_p - i\omega\mu_0(\nabla \times \mathbf{M}_p)$$

- **Homogeneous Dirichlet boundary condition:**

$$\mathbf{E} = 0 \qquad at\ \infty$$

or

$$\mathbf{E} \cdot \tau = 0 \qquad on\ \Gamma$$

- **Integral form of Maxwell's equations:**

$$\oint_{\partial S^D} \mathbf{E} \cdot d\mathbf{l}^D = -i\mu_0\omega \iint_{S^D} \mathbf{H} \cdot d\mathbf{S}^D - i\mu_0\omega \iint_{S^D} \mathbf{M}_p \cdot d\mathbf{S}^D$$

$$\oint_{\partial S^V} \mathbf{H} \cdot d\mathbf{l}^V = \sigma \iint_{S^V} \mathbf{E} \cdot d\mathbf{S}^V + \iint_{S^V} \mathbf{J}_p \cdot d\mathbf{S}^V$$

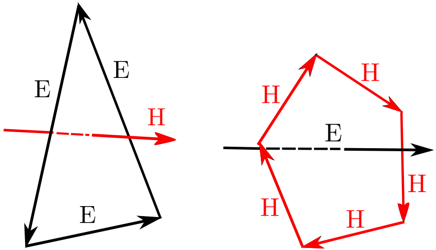

- **Discretized form of Maxwell's equations:**

$$\sum_{q=1}^{W_j^D} E_{i(j,q)}\, l_{i(j,q)}^D = -i\mu_0\omega H_j\, S_j^D - i\mu_0\omega M_{p_j}\, S_j^D$$

$$\sum_{k=1}^{W_i^V} H_{j(i,k)}\, l_{j(i,k)}^V = \sigma E_i\, S_i^V + J_{p_i}\, S_i^V .$$

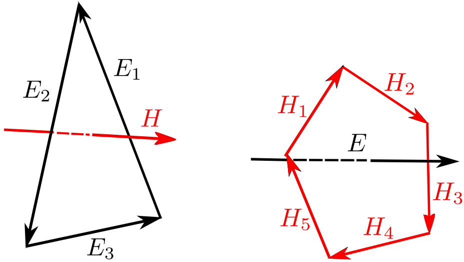

EM-field formulation: Discretization

- **Discretized form of Helmholtz equation:**

$$\sum_{k=1}^{W_i^V}\left(\left(\sum_{q=1}^{W_j^D} E_{i(j,q)}\, l^D_{i(j,q)}\right)\frac{l^V_{j(i,k)}}{S^D_{j(i,k)}}\right) + i\omega\mu_0\sigma E_i\, S_i^V$$

$$= -i\omega\mu_0 \sum_{k=1}^{W_i^V} M_{p_{j(i,k)}} \frac{l^V_{j(i,k)}}{S^D_{j(i,k)}} - i\omega\mu_0 J_{p_i}$$

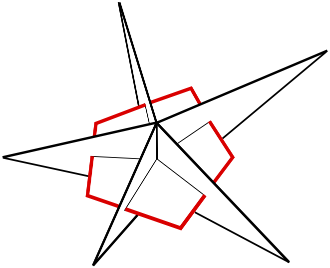

EM potential (A-ϕ) formulation of Maxwell's equations

- **Magnetic vector and electric scalar potentials:**

$$\mathbf{E} = -i\omega\mathbf{A} - \nabla\phi$$
$$\mu_0\mathbf{H} = \nabla \times \mathbf{A}$$

Helmholtz equation in terms of potentials with Coulomb gauge

$$\nabla \times \nabla \times \mathbf{A} - \nabla(\nabla \cdot \mathbf{A}) + i\omega\mu_0\sigma\mathbf{A} + \sigma\mu_0\nabla\phi = \mu_0\mathbf{J}_p + \mu_0\nabla \times \mathbf{M}_p$$

Conservation of charge

$$-\nabla \cdot \mathbf{J} = \nabla \cdot \mathbf{J}_p$$
$$i\omega\nabla \cdot \sigma\mathbf{A} + \nabla \cdot \sigma\nabla\phi = \nabla \cdot \mathbf{J}_p$$

- **Homogeneous Dirichlet boundary condition:**

$$(\mathbf{A}, \phi) = 0 \qquad at\ \infty$$

or

$$(\mathbf{A} \cdot \tau, \phi) = 0 \qquad on\ \Gamma$$

EM potential (A-ϕ) formulation of Maxwell's equations

Relations used for the finite-volume discretization

$$\nabla \times \mathbf{H} - \mu_0^{-1}\nabla\psi + i\omega\sigma\mathbf{A} + \sigma\nabla\phi = \mathbf{J}_p + \nabla \times \mathbf{M}_p \quad (1)$$

$$\mu_0\mathbf{H} = \nabla \times \mathbf{A} \quad (2)$$

$$\psi = \nabla \cdot \mathbf{A} \quad (3)$$

$$i\omega\nabla \cdot \sigma\mathbf{A} + \nabla \cdot \sigma\nabla\phi = \nabla \cdot \mathbf{J}_p \quad (4)$$

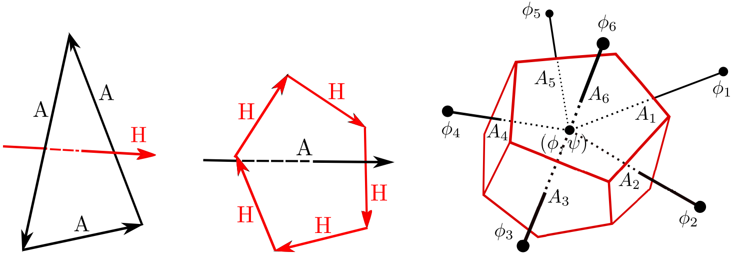

- **Decompose A and ϕ into real and imaginary parts:**

$$A = A_{re} + iA_{im} \;\; ; \;\; \phi = \phi_{re} + i\phi_{im}$$

- **Resulting block matrix equation:**

$$\begin{pmatrix} \mathbf{A} & -\omega\mathbf{B} & \mathbf{C} & 0 \\ \omega\mathbf{B} & \mathbf{A} & 0 & -\mathbf{C} \\ 0 & -\omega\mathbf{D} & \mathbf{E} & 0 \\ \omega\mathbf{D} & 0 & 0 & \mathbf{E} \end{pmatrix} \begin{pmatrix} \mathbf{A}_{re} \\ \mathbf{A}_{im} \\ \Phi_{re} \\ \Phi_{im} \end{pmatrix} = \begin{pmatrix} \mathbf{S}_1 \\ 0 \\ \mathbf{S}_2 \\ 0 \end{pmatrix}$$

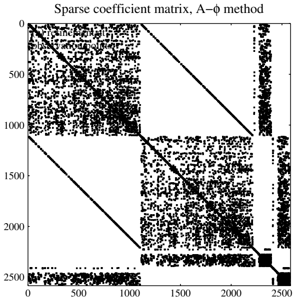

Solution of the finite-volume schemes

- **Direct solution: MUMPS sparse direct solver (Amestoy et. al, 2006)**
- **Iterative solution: BiCGSTAB and GMRES solvers from SPARSKIT (Saad, 1990)**

Example 1: grounded wire

- 100 m wire along the x axis operating at 3 Hz
- Dimensions of the prism: $120 \times 200 \times 400$ m
- $\sigma_{ground} = 0.02\ S/m$; $\sigma_{prism} = 0.2\ S/m$
- Observation points along the x axis

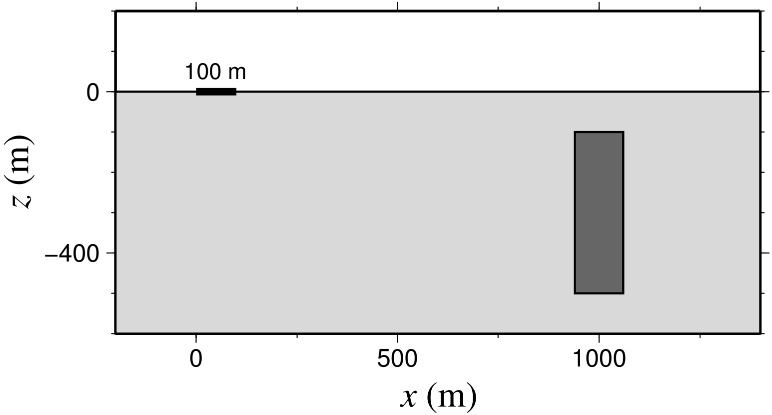

Example 1: grounded wire

- Dimensions of the domain: $40 \times 40 \times 40$ *km*
- Number of tetrahedra: 162,689

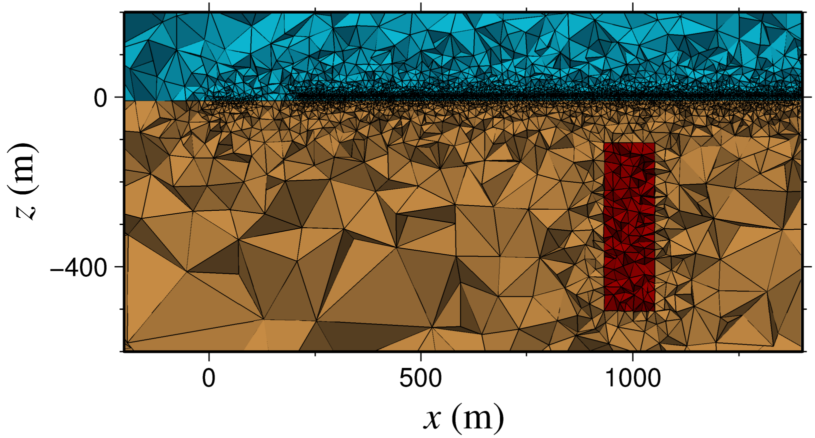

Example 1: grounded wire

- (on Apple Mac Pro; 2.26 GHz Quad-Core Intel Xeon processor)

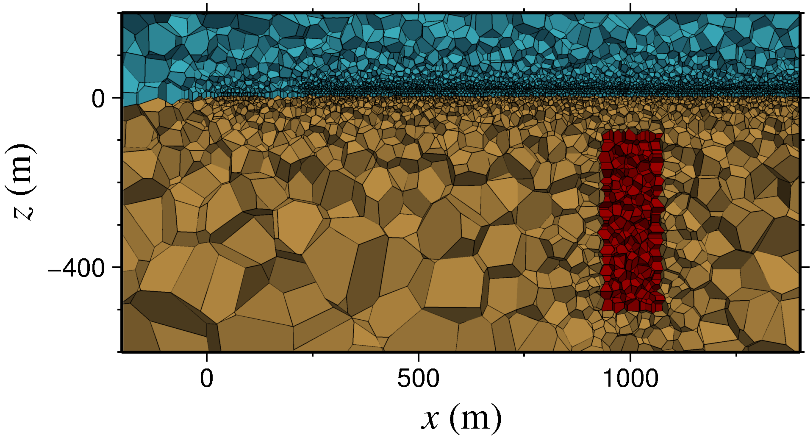

- Scattered electric field

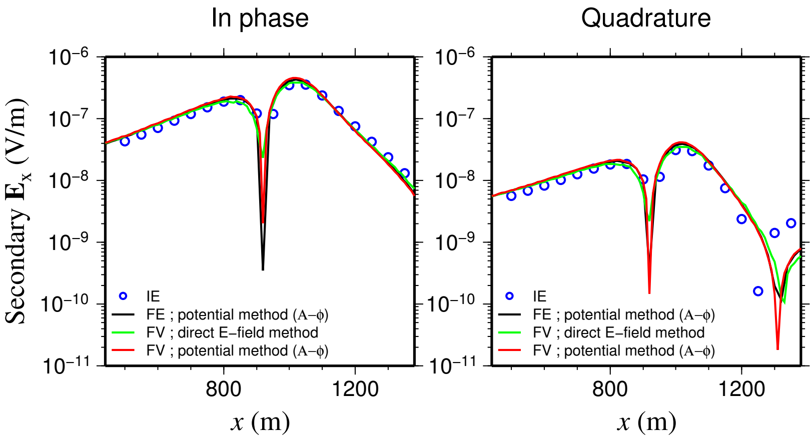

Example 1: grounded wire

- Galvanic part $(-\nabla\phi)$
- Inductive part $(-i\omega A)$
- Total electric field: $E = -\nabla\phi - i\omega A$

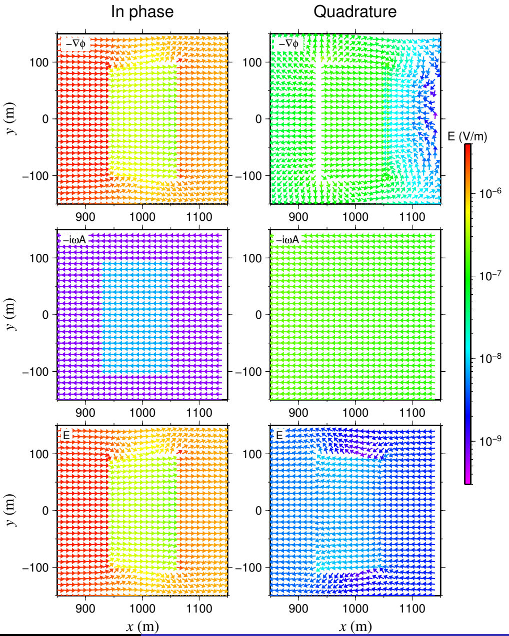

Example 1: grounded wire

- Galvanic part $(-\sigma\nabla\phi)$
- Inductive part $(-i\omega\sigma A)$
- Total current density: $J = -\sigma\nabla\phi - i\omega\sigma A$

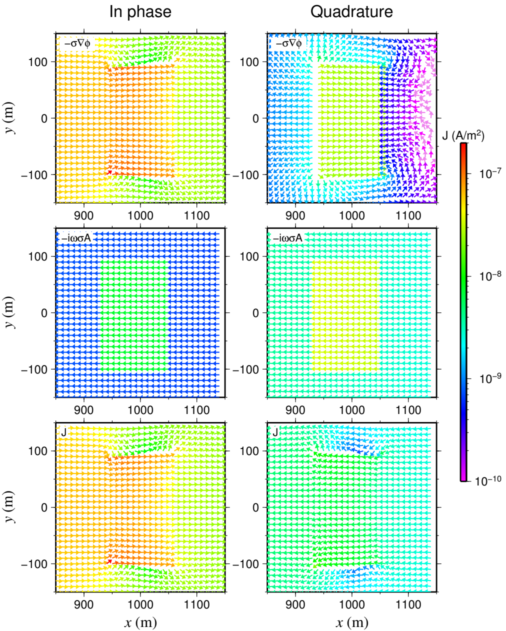

- Cumulative error versus the changing cell size at the observation points

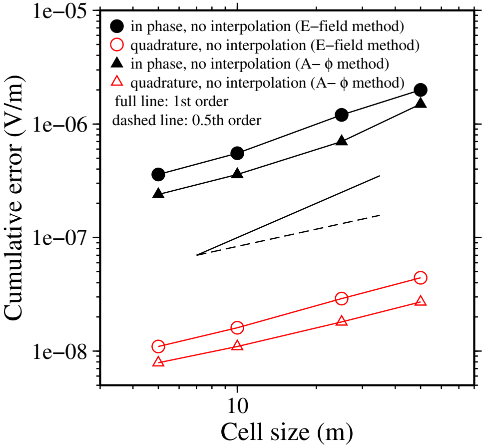

Example 1: grounded wire

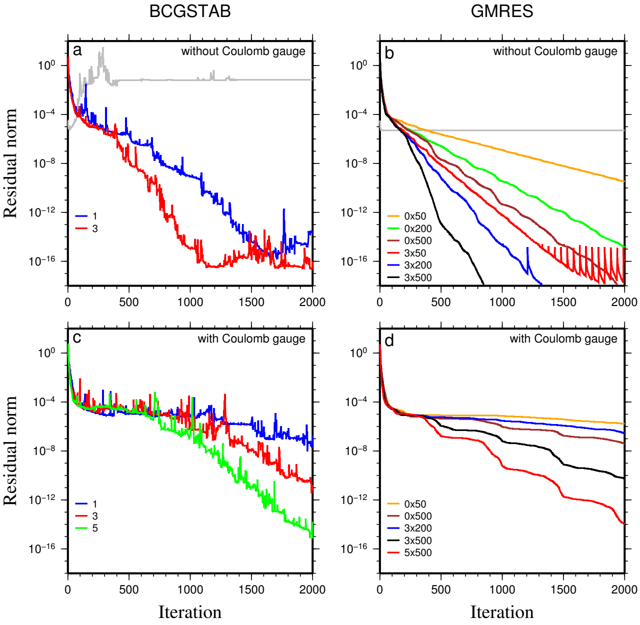

Example 2: Ovoid, HEM survey

- Ovoid: massive sulfide ore body, Voisey's Bay, Labrador, Canada
- HEM survey of the region has been simulated
- Transmitter and receiver towed below the helicopter 30 m above ground
- Transmitter-receiver separation was 8 m and the frequencies were 900 and 7200 Hz
- $\sigma_{ground} = 0.001$ and $\sigma_{ovoid} = 100$ S/m were chosen by try-and-error
- Number of tetrahedra: $240,692$

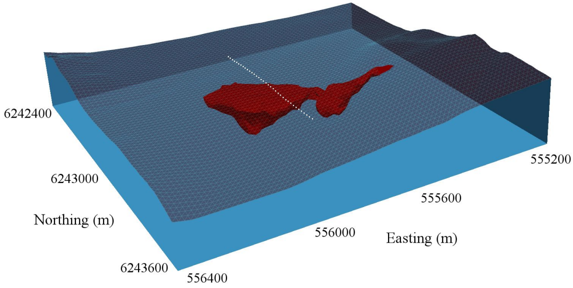

Example 2: Ovoid, HEM survey

- Topography of the region

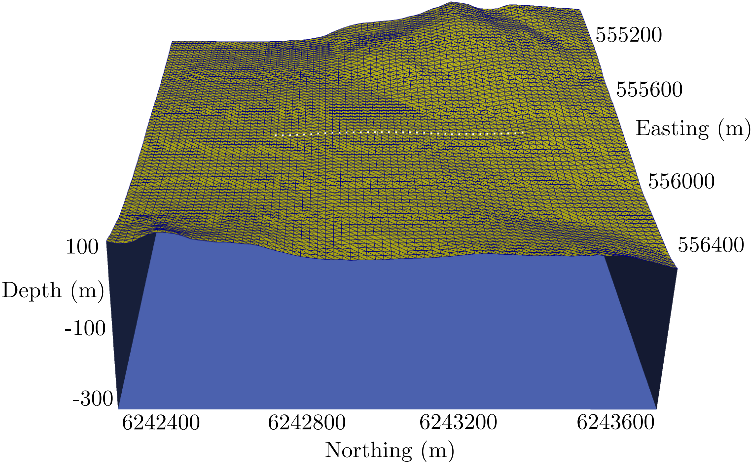

Example 2: Ovoid, HEM survey

- White dots show the observation points

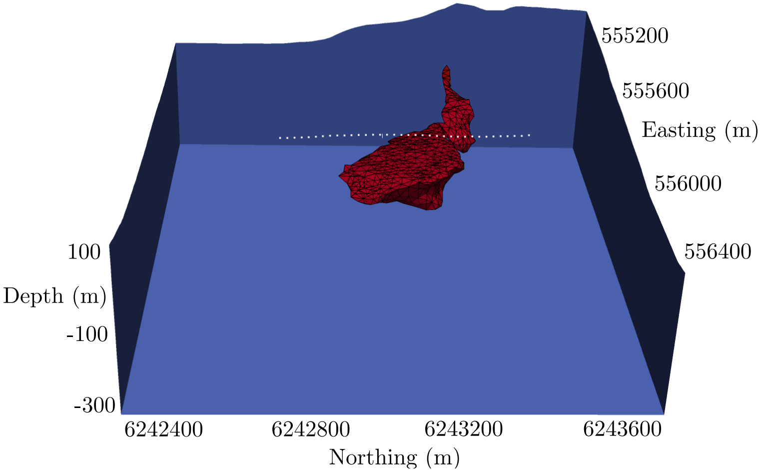

Example 2: Ovoid, HEM survey

- The plan view

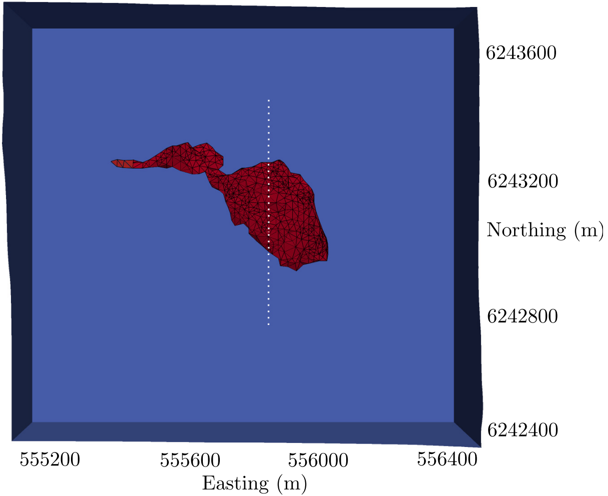

Example 2: Ovoid, HEM survey

- Grid refined at the sources and observation points

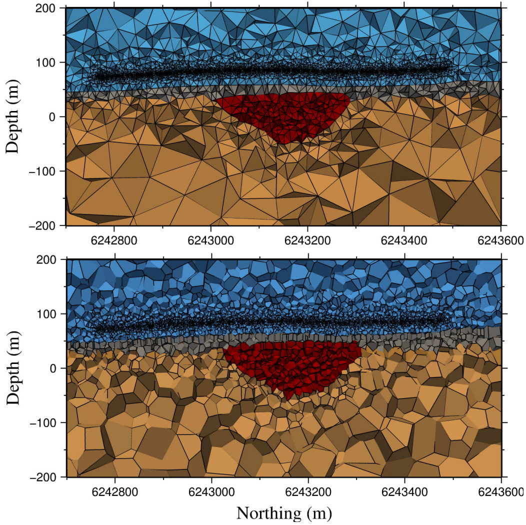

Example 2: Ovoid, HEM survey

- FV results (circles) vs real HEM data (lines)

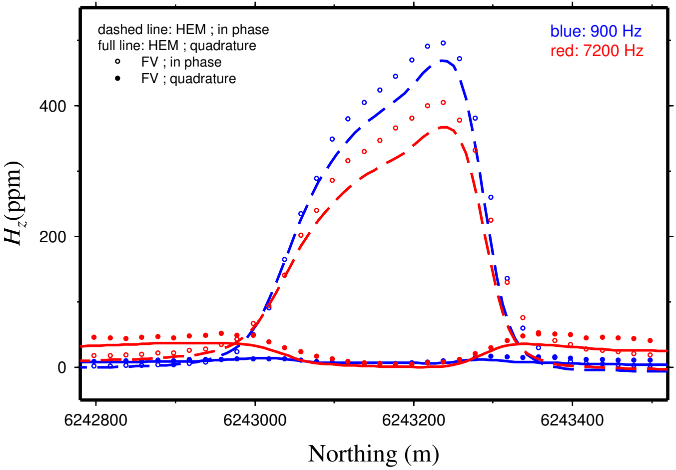

- Amplitude of the horizontal component of total current density at a vertical section along the observation profile

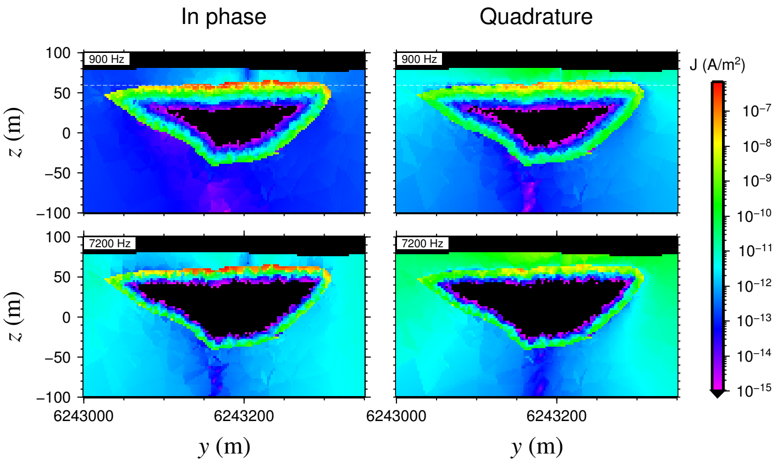

- Galvanic part ($-\sigma\nabla\phi$)
- Inductive part ($-i\omega\sigma A$)
- Total current density: $J = -\sigma\nabla\phi - i\omega\sigma A$

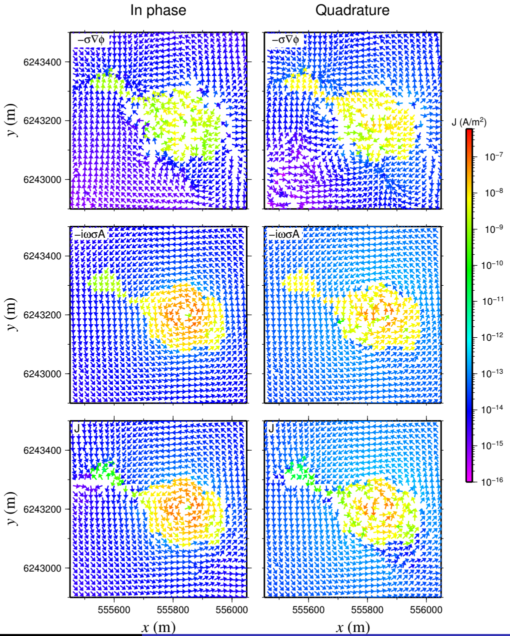

- A finite-volume approach was used for modelling total field EM data. It used staggered tetrahedral-Voronoï grids.
- The potential formulation of Maxwell's equation was discretized and solved and compared to the solution of the EM-field formulation.
- Accuracy and versatility were tested using two examples: one with a grounded wire source and a small conductivity contrast; another one with a realistic body, magnetic sources and a large conductivity contrast.
- Unlike the EM-field scheme, the $A - \phi$ scheme could be solved using generic iterative solvers.
- The gauged problems were harder to solve than the ungauged problems.
- Solutions were decomposed into galvanic and inductive parts. The results were in good agreement with the type of sources that were used.
- While both EM-field and potential schemes possessed the same trends of accuracy, the potential approach showed lower cumulative errors.

Acknowledgements

- ACOA
  (Atlantic Canada Opportunities Agency)

- NSERC
  (Natural Sciences and Engineering Research Council of Canada)

- Vale

Atlantic Canada Opportunities Agency

NSERC CRSNG

VALE

References

- Amestoy, P. R., Guermouche, A., L'Excellent, J. -Y. and S. Pralet, 2006. Hybrid scheduling for the parallel solution of linear systems, Parallel Computing, 32, 136156.
- Ansari, S. M., and C. G. Farquharson, 2013, Three-dimensional modeling of controlled-source electromagnetic response for inductive and galvanic components: Presented at the 5th International Symposium on Three-Dimensional Electromagnetics.
- Farquharson, C. G., and D. W. Oldenburg, 2002, An integral-equation solution to the geophysical electromagnetic forward-modelling problem, in Three-Dimensional Electromagnetics: Proceedings of the Second International Symposium: Elsevier, 319.
- Farquharson, C. G., Duckworth, K. and D. W. Oldenburg, 2006. Comparison of integral equation and physical scale modeling of the electromagnetic responses of models with large conductivity contrasts, Geophysics, 71, G169-G177.
- Madsen, N. K., and R. W. Ziolkowski, 1990, A three-dimensional modified finite volume technique for Maxwell's equations: Electromagnetics, 10, 147-161.
- Si, H., 2004. TetGen, a quality tetrahedral mesh generator and three-dimensional delaunay triangulator, v1.3 (Technical Report No. 9). Weierstrass Institute for Applied Analysis and Stochastics.
- Saad, Y., 1990. SPARSKIT: a basic tool kit for sparse matrix computations. Report RIACS 90-20, Research Institute for Advanced Computer Science. NASA Ames Research Center.